Origin of the Enhanced Catalytic Activity of Carbon Nanocoil-Supported PtRu Alloy Electrocatalysts

Kyung-Won Park[†] and Yung-Eun Sung*

Department of Materials Science & Engineering, Kwangju Institute of Science & Technology, Gwangju 500-712, Korea

Sangjin Han, Youngkwang Yun, and Taeghwan Hyeon

National Creative Research Initiative Center for Oxide Nanocrystalline Materials and School of Chemical Engineering, Seoul National University, Seoul 151-744, Korea

Received: September 18, 2003; In Final Form: November 10, 2003

The origin of the excellent electrocatalytic performance of PtRu alloy catalysts supported on newly synthesized carbon nanocoil supports was investigated. Among three commercially available carbon materials—Vulcan XC-72, multiwall carbon nanotube, and activated carbon, the Vulcan XC-72-supported catalyst exhibited the best catalytic performance. Carbon nanocoils with variable surface areas and crystallinity were employed as the supports for 60 wt % Pt/Ru (1:1) catalysts. The catalysts supported on all these three carbon nanocoils exhibited better electrocatalytic performance compared to the catalyst supported on Vulcan XC-72 carbon. In particular, the PtRu alloy catalyst supported on CNC-2, which has both good crystallinity and a large surface area, showed a superior electrocatalytic performance, compared to the catalysts supported on CNC-1 and CNC-3 carbons.

Introduction

Carbon is an ideal material for supporting nanosized metallic particles in the electrode for low-temperature fuel cells, such as polymer electrolyte membrane fuel cells.[1−3] No other materials except carbon material have the essential properties of electronic conductivity, corrosion resistance, surface properties, and the low cost required for the commercialization of fuel cells. The requirements of carbon materials for their applications to the supports for platinum-based electrocatalyst are as follows: a high surface area for a high level of dispersion of nanosized catalysts, excellent crystallinity or low electrical resistance to facilitate electron transport during the electrochemical reactions, a pore structure suitable for maximum fuel contact and byproduct release, and good interactions between the catalyst nanoparticles and the carbon support. However, it is extremely difficult to design and synthesize carbon materials with all these characteristics, particularly with both a high surface area and good crystallinity. Accordingly, in terms of the design and application of a catalyst support in fuel cells, novel carbon materials, that possess a high surface area, a well-defined porosity, and good crystallinity represent an attractive goal.

Many nanostructured carbon materials with graphitic framework structures, including the currently popular carbon nanotubes, have been intensively studied. These nanostructured carbon materials exhibit many interesting characteristics and have been applied extensively in various areas, including electron field emitters, catalytic supports, nanocomposites, quantum electronic devices, and electrode materials.[4−11] The synthetic methods of these nanostructured carbon materials include arc discharge, laser evaporation, and thermal chemical vapor deposition.[12−14] However, these synthetic methods have limitations in terms of commercial production because of the harsh synthetic conditions required and the low production yields. Taking these drawbacks into consideration, a solid-phase synthetic procedure might be more desirable. Although several groups reported on the solid-phase synthesis of nanostuctured carbon materials, the synthetic procedure often requires a long reaction time or a complicated series of synthetic steps.[15−17]

Direct methanol fuel cells (DMFCs),[18] which directly use methanol as fuel, have recently been studied intensively because of their numerous advantages that include high energy density, ease of handling a liquid, low operating temperatures, and their possible applications to micro-fuel cells.[19] The performance and stability of low-temperature fuel cells such as DMFCs are known to be strongly dependent on the carbon support used, as well as the catalytically active species.[20] Accordingly, it is important that a suitable carbon material for use as a catalyst support for DMFC systems need to be developed. Very recently, we have developed a new carbon nanocoil material and successfully applied the material for the catalysts support for DMFC electrodes.[21] Here we report on the detailed studies on the relationship between the electrocatalytic performance of PtRu catalysts and the characteristics of the carbon supports.

Experimental Section

Synthesis of Carbon Nanocoils (CNCs). The detailed synthetic procedure for the carbon nanocoils (CNCs) is described in the previous report.[21] In a typical procedure, a cobalt salt and a nickel salt were dissolved in 100 mL of a mixture aqueous solution including formaldehyde, and silica. After that, resorcinol was dissolved in the mixture solution. CNC-1 was synthesized

* Author to whom correspondence should be addressed. E-mail: ysung@kjist.ac.kr.

[†] Research Center for Energy Conversion and Storage, Seoul National University, Seoul 151-744, Korea.

10.1021/jp0368031 CCC: $27.50
Published on Web 12/24/2003

by the molar ratio of 100 H_2O/0.2 cobalt salt/0.2 nickel salt/1 resorcinol/2 formaldehyde. CNC-2 was synthesized by the molar ratio of 100 H_2O/0.4 cobalt salt/0.4 nickel salt/1 resorcinol/2 formaldehyde/0.6 silica. CNC-3 was synthesized by the molar ratio of 100 H_2O/0.2 cobalt salt/0.2 nickel salt/1 resorcinol/2 formaldehyde/0.6 silica. The resulting reaction mixture was cured at 85 °C for 3 h in a closed system. For the carbonization, the composite was heated under a nitrogen atmosphere from room temperature to 900 °C at a heating rate of 3 °C min^{-1} and then held at this temperature for 6 h. The resulting composites were then stirred in 3 M NaOH solutions for 3 h to remove silica particles, followed by refluxing in 2.5 M HNO_3 solution for 6 h to remove metal particles, resulting in the formation of carbon nanocoils (CNCs).

Characterization of Materials. The X-ray diffraction (XRD) patterns were obtained on a Rigaku X-ray diffractometer equipped with a Cu Kα source and operating at 40 kV and 40 mA. To estimate the size and composition of the PtRu alloy particles, the (220) peak was fitted using the Lorentian/Gaussian function. The size and composition were obtained using the Debye−Scherrer equation and Vegard's law. The transmission electron microscopic (TEM) investigation was carried out using a Phillips CM20T/STEM electron microscope at an accelerating voltage of 200 kV. Specimens were prepared by ultrasonically suspending the particles in deionized water. Few drops of the suspensions were deposited on a standard Cu grid covered with a carbon film (200 mesh). Nitrogen adsorption/desorption isotherms were measured at 77 K using a Micromeritics ASAP 2000 system. Total surface area was determined using BET (Brunauer−Emmett−Teller) equation.

Preparation Method for Electrochemical Study. Carbon-supported catalysts were synthesized at room temperature by the conventional reduction method using a Pt salt ($H_2PtCl_6 \cdot 6H_2O$, Aldrich Chem. Co.), Ru salt($RuCl_3 \cdot xH_2O$, Aldrich Chem. Co.), and $NaBH_4$ as the reducing agent.[22,23] Electrochemical measurements were conducted using a three-electrode cell at 25 °C. A Pt gauze and an Ag/AgCl (in saturated KCl) were used as the counter and reference electrodes, respectively. The working carbon electrode (6 mm in diameter) was polished with 1, 0.3, and 0.05 μm Al_2O_3 paste and washed ultrasonically in Millipore water (18 MΩ·cm). The catalyst ink, consisting of the catalyst and the Nafion ionomer in water and 2-propanol was dropped on the working electrode, and dried at 70 °C in a vacuum oven. Solutions of 0.5 M H_2SO_4 and 2.0 M CH_3OH in 0.5 M H_2SO_4 were stirred constantly and purged with nitrogen gas. All chemicals used were of analytical grade. Electrochemical experiments were performed using an AUTOLAB instrument from Eco Chemie. To compare the catalytic activity of the supported catalysts with respect to methanol oxidation, voltammetry was performed in the potential range of 0−0.7 V vs NHE.[22] For a membrane-electrode-assembly (MEA) of DMFC, the anode (supported catalysts) of 2 mg of PtRu per cm^2 and cathode of 5 mg per cm^2 (Pt black, Johnson-Matthey Co.) catalyst layers were formed on Teflonized carbon paper (TGPH-090) substrates using catalyst inks containing the appropriate weight percent of Nafion ionomer solution (Aldrich. Co.). The MEA for unit cell tests were fabricated by pressing the as-prepared cathode and anode layers onto both sides of a pretreated Nafion 117 electrolyte membrane at 110 °C and 1000 psi for 3 min. Cell performance was evaluated by means of a DMFC unit cell with a 2 cm^2 cross-sectional area, and measured with a potentiometer, which recorded the cell under conditions of constant current.[24] Both fuel and oxidant flow paths were machined into graphite block end plates, which also served as current collectors. A 2 M methanol solution with a flow rate of 1 cm^3/min was supplied by a Masterflex liquid micro-pump, and dry O_2 flow was regulated at 500 cm^3/min using a flow meter.

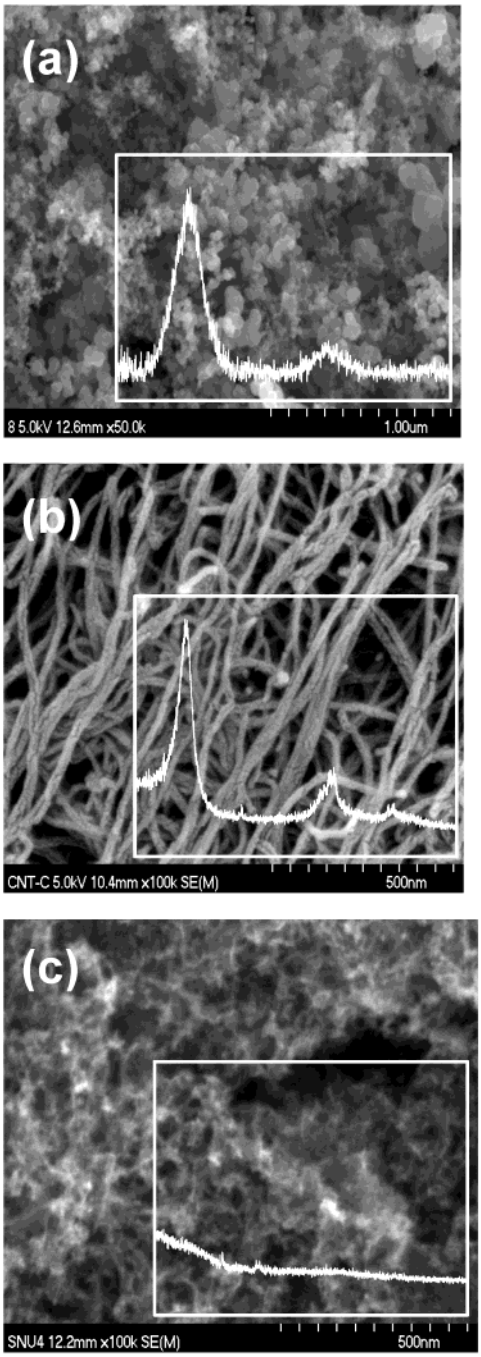

Figure 1. Scanning electron microscopy (SEM) images and X-ray diffraction (XRD) patterns of various carbons as candidates of supporting materials: (a) Vulcan XC-72, (b) multiwall carbon nanotube (CNT), and (c) activated carbon.

Results and Discussion

Figure 1 shows scanning electron microscopy (SEM) images and X-ray diffraction (XRD) patterns of various commercially available carbon materials that are used as catalyst supports in the current study. The carbon materials are Vulcan XC-72, multiwall carbon nanotubes, and activated carbon. The SEM image of Vulcan XC-72 carbon, which is the most widely used support material for direct methanol fuel cell electrodes, is

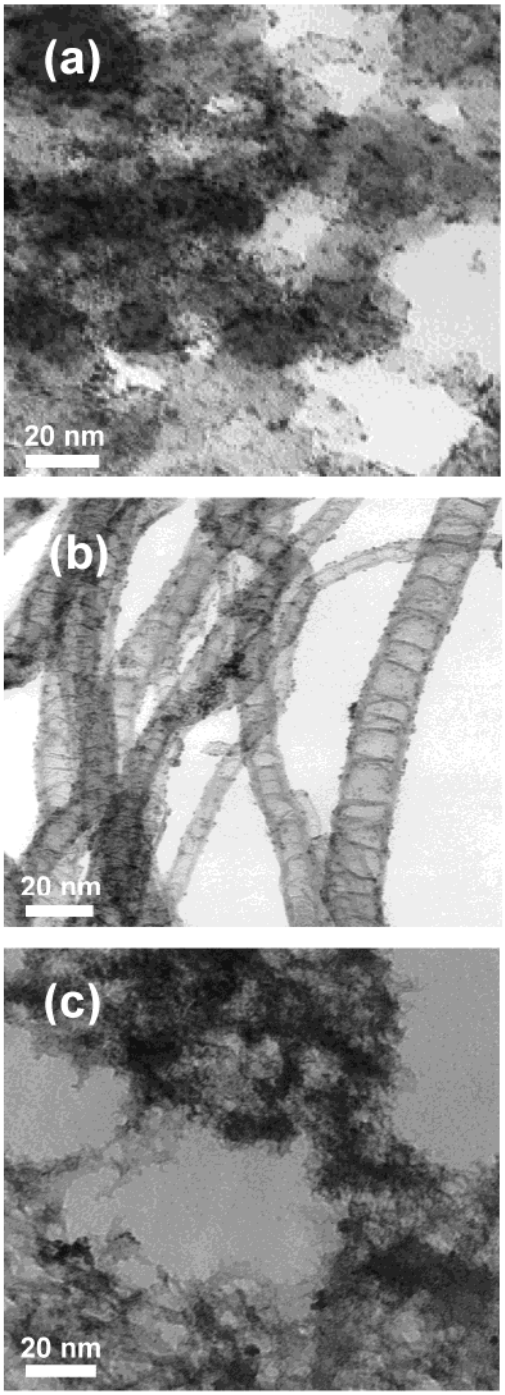

Figure 2. Transmission electron microscope (TEM) images of (a) Vulcan XC-72, (b) multiwall carbon nanotube (CNT), and (c) activated carbon-supported PtRu alloy electrocatalysts.

shown in Figure 1a. Vulcan XC-72 has a round particle shape with particle sizes of several tens of nanometers; however, the exact structure of the carbon particles is currently under debate. Carbon nanotubes (CNT), which are highly crystalline, are also tested as electrocatalyst support, because graphitic crystallinity is important for electron transport during the electrochemical reaction. A multiwall CNT prepared by means of a CVD process shows graphitic carbon with excellent crystallinity and a length of 10−50 μm and a diameter of 15−30 nm (Figure 1b). In addition, amorphous activated carbon with a high surface area of about 1000 m^2/g, which is important for the high dispersion of the nanosized catalysts, was employed as the catalyst support.

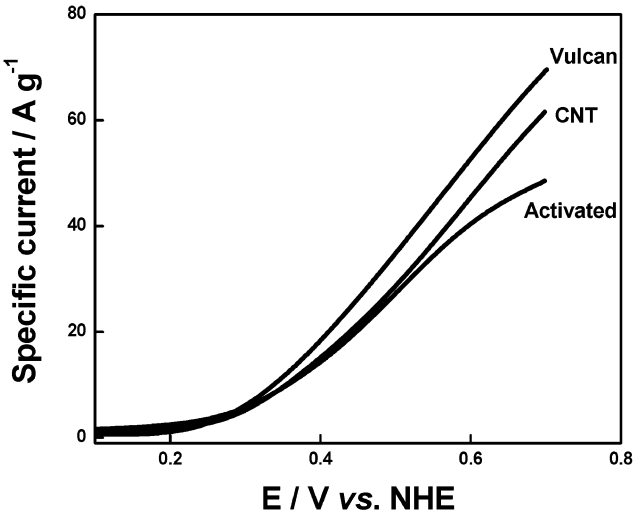

Figure 3. Comparison of catalytic activity with respect to the methanol electrooxidation of PtRu alloy electrocatalysts supported by (a) Vulcan XC-72, (b) multiwall carbon nanotube (CNT), and (c) activated carbon.

At first, the PtRu nanosized electrocatalysts for methanol electrooxidation in DMFC were prepared using the commercially available carbon materials. The TEM images of 60 wt % Pt/Ru (1:1) alloy catalysts supported on Vulcan XC-72, multiwall CNT, and amorphous activated carbon are shown in Figure 2a, b, and c, respectively. Whereas the catalysts supported on Vulcan XC-72 and multiwall CNT exhibited high dispersion of catalyst nanoparticles, the activated carbon-supported catalysts showed the extensive agglomeration of catalyst nanoparticles. To evaluate the electrocatalytic activity of carbon-supported catalysts, the methanol electrooxidation current of the catalysts was measured using a fundamental electrochemical system. The order of catalytic activity of the carbon-supported catalysts is Vulcan XC-72 > multiwall CNT > amorphous activated carbon, as shown in Figure 3. The lower catalytic activity of multiwall CNT-supported catalysts compared to that of the Vulcan XC-72-supported catalyst, despite the high electrical conductivity, seems to result from the lower effective surface area for the deposition of metal nanoparticles by comparing the active surface area of the supported catalysts, measured using CO chemisorption (Pt−CO) and the hydrogen adsorption/desorption (Pt−H) method.[21] The lower catalytic activity of the amorphous activated carbon-supported catalyst compared to that of the Vulcan XC-72-supported catalyst, despite the high surface area of activated carbon, seems to be caused by the poor electrical conductivity and the agglomeration of nanosized catalysts. Consequently, for a high electrocatalytic activity in carbon-supported nanosized electrocatalyst, the carbon material should have well-optimized properties with regard to high surface area and good crystallinity. Other desirable characteristics are good pore structures such as uniform pore size and good interaction between catalysts and carbon materials. However, it is well-known that it is extremely difficult to design carbon materials having both a high surface area and good crystallinity. Accordingly, the design of novel carbon materials for the applications for a catalyst support in fuel cell is needed.

We used three different carbon nanocoil materials for the elecrocatalyst support. Table 1 shows the characteristics of these three carbon nanocoils (CNCs) and Vulcan XC-72 carbon. As shown in Figure 4, the CNCs consist of the graphitic coils with a thickness of 5−10 nm. Figure 5 compares the XRD patterns of three different CNCs and Vulcan XC-72 carbon. The CNC-1 exhibits excellent graphitic properties with a (002) plane *d* spacing of 3.43 Å and clearly observed (100) and (004) peaks.

TABLE 1: Characteristics of Carbon Nanocoils (CNCs) for Use as Supporting Materials in a Direct Methanol Fuel Cell (DMFC)

	particle size (nm)	crystallinity	surface area (m^2/g)
CNC-1	5−10[a]	good	110
CNC-2	5−10[a]	good	318
CNC-3	5−10[a]	medium	451
Vulcan XC-72	20−40	amorphous	212

[a] The thickness of carbon nanocoil.

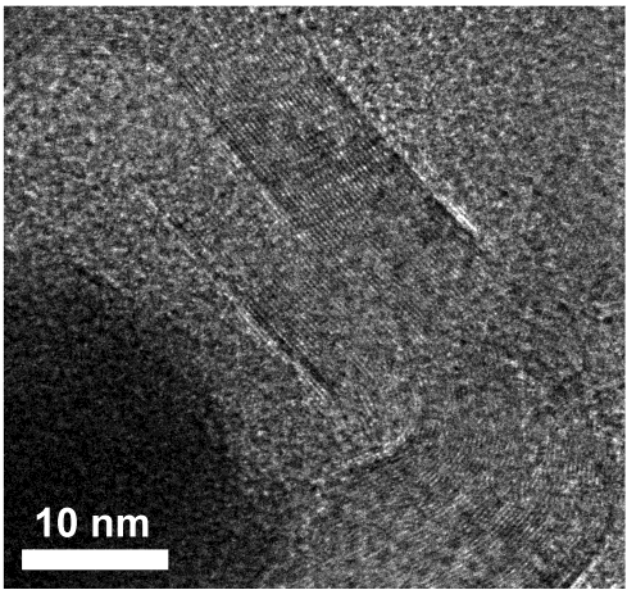

Figure 4. Transmission electron microscope (TEM) image of a carbon nanocoil (CNC).

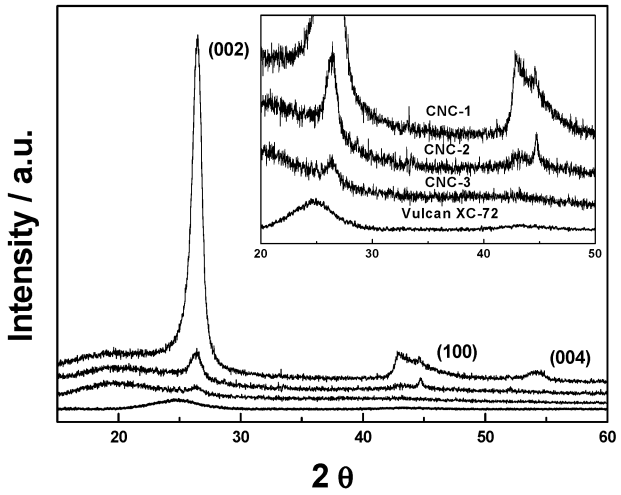

Figure 5. X-ray diffraction (XRD) patterns of well-controlled carbon nanocoil (CNC) supports.

The measured crystallite size of the individual nanocoil perpendicular to the basal plane (L_c), using the Debye−Scherrer formula, was calculated to be 7.8 nm and the BET surface area of CNC-1 is 110 m^2/g. On the other hand, CNC-3 shows a medium level of crystallinity, superior to that of amorphous Vulcan XC-72, with a high surface area of 451 m^2/g as shown in Figure 5 and Table 1. In addition, the CNC material showed a well-developed mesoporous structure measured by N_2 isotherm. In particular, CNC-2 has both a high surface area and excellent crystallinity, which are required for the supporting materials of an electrocatalyst and would be expected to have the good catalytic activity of a CNC-2-supported catalyst.

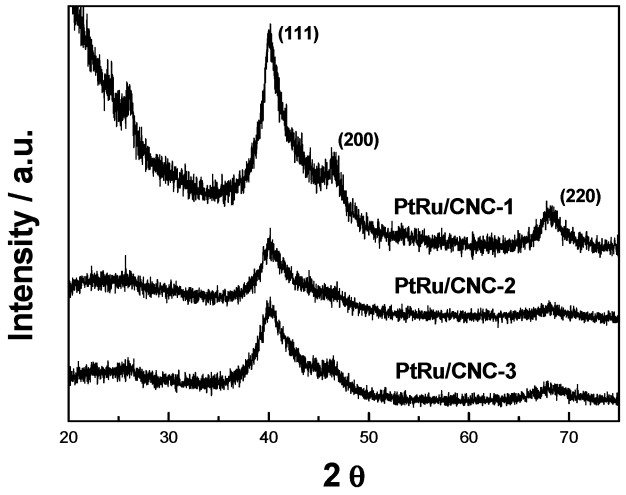

Figure 6. X-ray diffraction (XRD) patterns of PtRu alloy supported electrocatalyst on carbon nanocoil (CNC) supports.

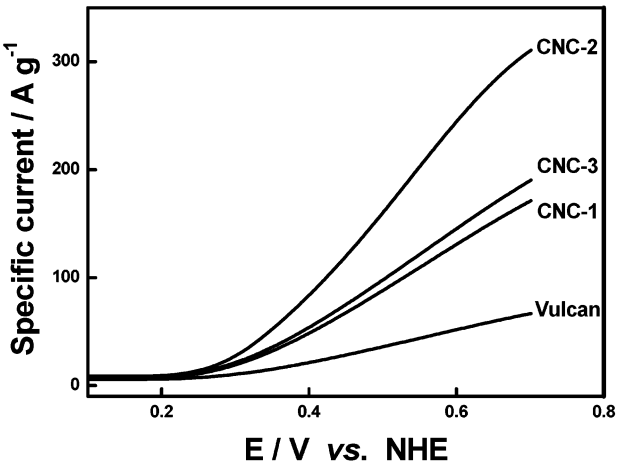

Figure 7. Plot of methanol electrooxidation versus applied potential of PtRu alloy electrocatalysts supported electrocatalyst on carbon nanocoils (CNCs) as supporting materials compared to Vulcan XC-72.

To investigate the possibility of using CNCs as an electrocatalyst support, the CNC-supported PtRu alloy catalysts were characterized by means of XRD analysis as shown in Figure 6. The particle size of PtRu (1:1) catalyst particles supported on these three CNCs, calculated by means of Vegard's law and the Debye−Scherrer equation from the XRD patterns, was similar with an average particle size of ∼2.5 nm. In addition, it was found that composition of Pt to Ru obtained by EDX and XPS analysis was in relatively good agreement with that confirmed by XRD pattern. In the XRD patterns, (111), (200), and (220) peaks from Pt-based fcc structure are evident, in addition to the main peaks from the carbon materials. A high catalyst loading of 60 wt %, confirmed by EDX and AAS-(Atomic Absorption Spectrophotometry) analysis, was applied because a high loading of Pt-based alloy catalyst is essential for the anode in DMFC. For a comparison of the catalytic activity of the supported catalyst on well-designed CNCs, the methanol electrooxidation specific current, that is, the current per gram of PtRu alloy catalyst, was measured as a function of applied potential in a typical electrochemical system. As shown in Figure 7, CNC-1, -2, and -3 show specific oxidation currents of 19, 27, and 21 A/g at 0.3 V versus NHE, respectively, compared to ∼12 A/g for Vulcan XC-72.[25] The PtRu alloy catalyst on CNC-2, which exhibited excellent crystallinity and a large surface area of 318 m^2/g, displays a higher specific

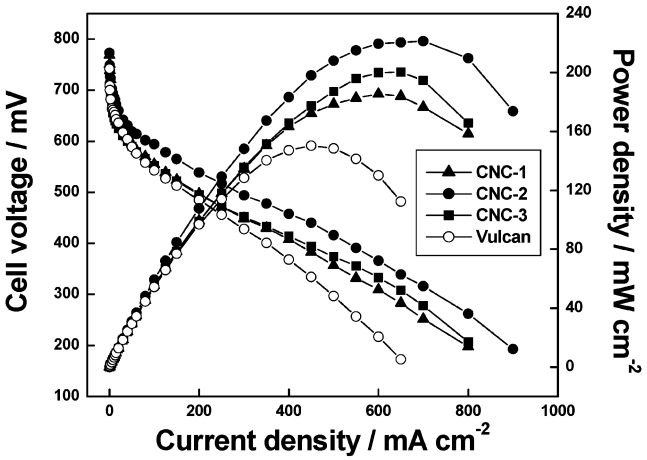

Figure 8. Polarization curves of direct methanol fuel cell using carbon nanocoil (CNC)-supported PtRu alloy electrocatalysts compared to Vulcan XC-72-supported PtRu alloy electrocatalyst at 60 °C.

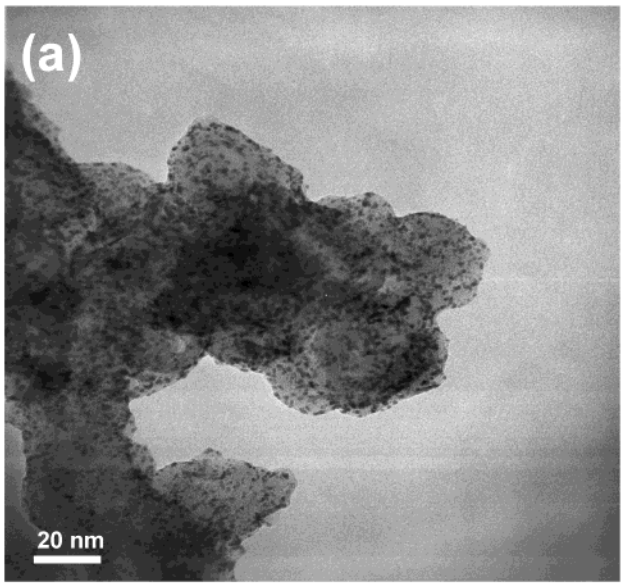

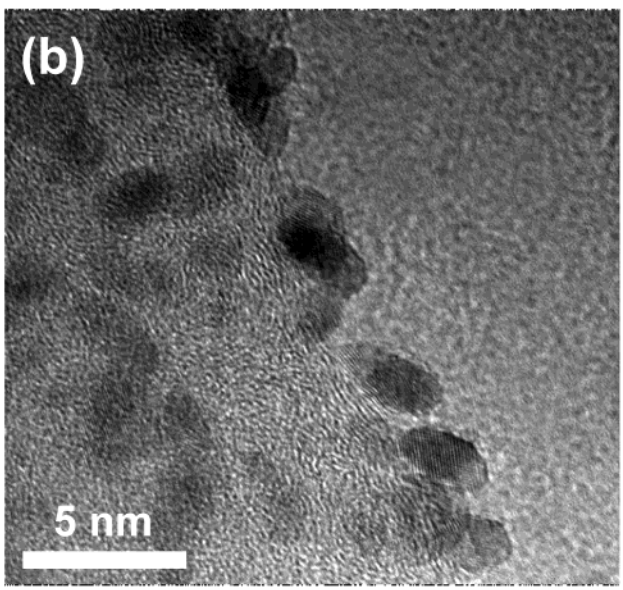

Figure 9. (a) Transmission electron microscope (TEM) and (b) high-resolution images of PtRu alloy electrocatalysts supported by carbon nanocoil (CNC-2).

current than that for CNC-1 and -3, which have a lower surface area and less graphitic structure, respectively. This indicates the excellent catalytic activity is directly related to the properties of the carbon materials such as crystallinity and surface area.

Another important measurement of catalytic performance of the CNC-supported PtRu catalysts is their applications to electrodes in a practical DMFC system. It is well-known that supported catalysts at low temperature have a major effect on the whole performance of a fuel cell. In particular, comparisons of DMFC performance are the most practical and powerful characterization method for comparing the catalytic activity of catalysts in an actual system. Figure 8 shows the polarization curves for a direct methanol fuel cell at 60 °C using carbon-supported catalysts as anode. The CNC-2-supported catalyst shows the highest current density at an activation polarization regime compared to catalysts supported on CNC-1 or 3 as well as Vulcan XC-72. Such an improved catalytic activity indicates that the use of CNC-2 can lead to a considerable reduction in the amount of catalyst used in a fuel cell. In addition, the unique pore structure of the support, which favors the diffusion of methanol fuel and the removal of the byproduct CO_2 gas, could be responsible for the improved fuel cell performance. The excellent performance of CNC-supported catalyst in the electrochemical half and single cell can be attributed to the superior dispersion of nanosized metallic nanoparticles on CNC as shown in Figure 9. In addition to dispersion effect of the support material, a good interaction between the support material and the metal catalyst particles seems to be also important. It has been reported that catalysts supported on carbon materials with specific characteristics such as a highly graphitic structure showed improved catalytic activities as a result of a preferred crystallographic orientation by interactions with the highly ordered substrate.[26] Detailed studies of the origins of interactions between the CNC support and PtRu alloy catalysts will be reported in the future.

Acknowledgment. This work was supported by KOSEF through the Research Center for Energy Conversion and Storage and the Brain Korea 21 project from the Ministry of Education. T.H. thanks the National Creative Research Initiative Program of the Korean Ministry of Science and Technology for financial support.

References and Notes

(1) Kinoshita, K. *Carbon, Electrochemical and Physicochemical Properties*; John Wiley & Sons: New York, 1998.

(2) Burchell, T. D. *Carbon Materials for Advanced Technologie*; Pergamon: New York, 1999.

(3) Marsh, H., Rodriguez-Reinoso, F., Eds. *Sciences of Carbon Materials*; Publicaciones de la Universidad de Alicante: Alicante, Spain, 1997.

(4) Subramoney, S. *Adv. Mater.* **1998**, *10*, 1157.

(5) Yoshimura, S.; Chang, R. P. H. *Supercarbon*; Springer: Berlin, 1998.

(6) Tománek, D.; Enbody, R. J. Kluwer: Dordrecht, 2000.

(7) Heer, W. A.; Chatelan, A.; Ugarte, D. *Science* **1995**, *270*, 1179.

(8) Planeix, J. M.; Coustel, N.; Coq, B.; Brotons, V.; Kumbhar, P. S.; Dutarte, R.; Geneste, P.; Bernier, P.; Ajayan, P. M. *J. Am. Chem. Soc.* **1994**, *116*, 7935.

(9) Gong, X.; Liu, J.; Baskaran, S.; Voise, R. D.; Young, J. S. *Chem. Mater.* **2000**, *12*, 1049.

(10) Hu, J.; Ouyang, M.; Yang, P.; Lieber, C. M. *Nature* **1999**, *399*, 48.

(11) Bessel, C. A.; Laubernds, K.; Rodriguez, N. M.; Baker, R. T. K. *J. Phys. Chem. B* **2001**, *105*, 1115.

(12) Ebbesen, T. W.; Ajayan, P. M. *Nature* **1992**, *358*, 220.

(13) Thess, A.; Lee, R.; Nikolaev, P.; Dai, H.; Petit, P.; Robert, J.; Xu, C.; Lee, Y. H.; Kim, S. G.; Rinzler, A. G.; Colbert, D. T.; Scuseria, G. E.; Tomanek, D.; Fischer, J. E.; Smalley, R. E. *Science* **1996**, *273*, 483.

(14) Fan, S.; Chapline, M. C.; Frankin, N. R.; Tombler, T. W.; Cassell, A. M.; Dai, H. *Science* **1999**, *283*, 512.

(15) Cho, W.; Hanada, E.; Kondo, Y.; Takayanagi, K. *Appl. Phys. Lett.* **1996**, *69*, 278.

(16) Kiselev, N. A.; Sloan, J.; Zakharov, D. N.; Kukovitskii, E. F.; Hutchison, J. L.; Hammer, J. A.; Kotosonov, S. *Carbon* **1998**, *36*, 1149.

(17) Maladonado-Hodar, F. J.; Moreno-Castilla, C.; Rivera-Utrilla, J.; Hanazawa, Y.; Yamada, Y. *Langmuir* **2000**, *16*, 4367.

(18) (a) Reddington, E.; Sapienza, A.; Gurau, B.; Viswanathan, R.; Sarangapani, S.; Smotkin, E. S.; Mallouk, T. E. *Science* **1998**, *280*, 1735. (b) Gurau, B.; Viswanathan, R.; Liu, R.; Lafrenz, T. J.; Ley, K. L.; Smotkin, E. S.; Reddington, E.; Sapienza, A.; Chan, B. C.; Mallouk, T. E.; Sarangpani, S. *J. Phys. Chem. B* **1998**, *102*, 9997. (c) Ross, P. N. In *Electrocatalysis*; Lipkowski, J., Ross, P. N., Eds.; Wiley-VCH: New York, 1998; Chapter 2. (d) Wieckowski, A., Ed. In *Interfacial Electrochemistry*; Marcel-Dekker: New York, 1999; Chapters 44−51.

(19) (a) Park, K.-W.; Ahn, K.-S.; Choi, J.-H.; Nah, Y.-C.; Kim, Y.-M.; Sung, Y.-E. *Appl. Phys. Lett.* **2002**, *81*, 907. (b) Park, K.-W.; Ahn, K.-S.; Choi, J.-H.; Nah, Y.-C.; Sung, Y.-E. *Appl. Phys. Lett.* **2003**, *82*, 1090. (c) Park, K.-W.; Choi, J.-H.; Sung, Y.-E. *J. Phys. Chem. B* **2003**, *107*, 5851.

(20) (a) Steigerwalt, E. S.; Deluga, G. A.; Cliffel, D. E.; Lukehart, C. M. *J. Phys. Chem. B* **2001**, *105*, 8097. (b) King, W. D.; Corns, J. D.; Murphy, O. J.; Boxall, D. L. E.; Kenik, A.; Kwiatkowski, K. C.; Stock, S. R.; Lukehart, C. M. *J. Phys. Chem. B* **2003**, *107*, 5467.

(21) (a) Hyeon, T.; Han, S.; Sung, Y.-E.; Park, K.-W.; Kim, Y.-W. *Angew. Chem. Int. Ed.* **2003**, *42*, 4352. (b) Han, S.; Yun, Y.; Park, K.-W.; Sung, Y.-E.; Hyeon, T. *Adv. Mater.* **2003**, *15*, 1922.

(22) (a) Lee, S.-A.; Park, K.-W.; Kwon B.-K.; Sung, Y.-E. *J. Electrochem. Soc.* **2002**, *149*, 1299. (b) Park, K.-W.; Choi, J.-H.; Kwon, B.-K.; Lee, S.-A.; Sung, Y.-E.; Ha, H.-Y.; Hong, S.-A.; Kim, H.; Wieckowski, A. *J. Phys. Chem. B* **2002**, *106*, 1869.

(23) Kinoshita, K.; Stonehart, P. *Modern Aspect of Electrochemisty*; Plenum Press: New York, 1996; 12.

(24) (a) Park, K.-W.; Ahn, H.-J.; Sung, Y.-E. *J. Power Sources* **2002**, *109*, 500. (b) Park, K.-W.; Kwon, B.-K.; Choi, J.-H.; Park, I.-S.; Kim, Y.-M.; Sung, Y.-E. *J. Power Sources* **2002**, *109*, 439.

(25) (a) Schmidt, T. J.; Gasteiger, H. A.; Behm, R. J. *Electrochem. Commun.* **1999**, *1*, 1. (b) Hamnett, A.; Weeks, S. A.; Kennedy, B. J.; Troughton, G.; Christensen, P. A. *Ber. Bunsen-Ges. Phy. Chem.* **1990**, *94*, 1014.

(26) (a) Park, C.; Baker, R. T. K. *J. Phys. Chem. B* **1998**, *102*, 5168. (b) Bessel, C. A.; Laubernds, K.; Rodriguez, N. M.; Baker, R. T. K. *J. Phys. Chem. B* **2001**, *105*, 1115.